Unexpected Magnetic Properties of Gas-Stabilised Platinum Nanostructures in the Tunneling Regime

Oscar Céspedes, [1,2*] *May Wheeler,*[1] *Timothy Moorsom*[1] *and Michel Viret*[2]

[1]School of Physics and Astronomy, University of Leeds, LS2 9JT, U.K.

[2]Service de Physique de l'Etat Condensé, DSM/IRAMIS/SPEC, CEA Saclay, CNRS URA 2464, F-91191 Gif-Sur-Yvette, France

Nanostructured materials often have properties widely different from bulk, imposed by quantum limits to a physical property of the material. This includes, for example, superparamagnetism and quantized conductance, but original properties such as magnetoresistance in non-magnetic molecular structures may also emerge. In this letter, we report on the atomic manipulation of platinum nanocontacts in order to induce magnetoresistance. Platinum is a paramagnetic 5d metal, but atomic chains of this material have been predicted to be magnetically ordered with a large anisotropy. Remarkably, we find that a gas flow stabilizes Pt atomic structures in a break junction experiment, where we observe extraordinary resistance changes over 30,000% in a temperature range up to 77 K. Simulations indicate that this behavior may stem from a previously unknown magnetically ordered, low-energy state in platinum oxide atomic chains. This is supported by measurements in Pt/PtOx superlattices revealing the presence of a ferromagnetic moment. These properties open new paths of research for atomic scale "dirty" magnetic sensors and quantum devices.

Keywords: Magnetoresistance, Platinum Oxide, Nanocontact, Spin Dependent Tunneling

Calculations suggest that platinum atomic chains of 1 nm or longer should exhibit spontaneous Hund's rule superparamagnetism at low temperature .[1-4] This would imply that the spins can be frozen in a direction determined by an external magnetic field. Moreover, the conductance of a single Pt atomic contact is dominated by conducting channels defined by the 8 valence electrons, and it is expected to vary as a function of the chain length and interatomic distance.[1, 3, 5] In ideal magnetic atomic structures only one spin channel may be available, so that the conductance can vary in multiples of e^2/h ($G_0/2$). Structures with a resistance above 25.9 kΩ (h/e^2) have little or no orbital overlap, and therefore electrons must tunnel between the atoms forming the chain. In this context, fractional conductance peaks have been observed for Pd and Pt atomic contacts, and have been attributed to spin polarized transport.[6] However, these results are not necessarily a proof of magnetic ordering, since the observed conductance peaks around e^2/h are rather broad and may have been caused by several sub-optimal conducting channels. In fact, fractional conduction peaks have been found in Pt and Au wires contaminated by molecules.[7, 8] Shot noise measurements in pure Pt atomic chains have given evidence for a non-magnetic ground state, but this discrepancy with the theory could be due to spin polarized electrons that do not contribute to the transport.[9] Molecular structures can show large magnetoresistance (MR) and quantum interference,[10-12] and a positive MR has been observed at low temperatures in Pd atomic structures.[13] Platinum electrodes have also been considered for highly conducting molecular scale junctions.[14] These highly responsive devices could be thought of as magnetic sensors with potential application in nanoscale memory storage. Furthermore, the possibility of a spin structure where the strength and time scale of the magnetic interactions are controlled at the atomic scale via electromagnetic fields could be the electronic equivalent to optical devices in

quantum computing. Manipulation of the contact structure could also result in changes of conductance, Kondo effect and magnetic ordering.[15-17]

Here, we study atomic contacts of Pt fabricated using the break junction technique.[18, 19] Pt films for break junctions were deposited using e-beam evaporation from targets containing less than 1 ppm magnetic impurities. The devices were fabricated via lift-off from e-beam patterned PMMA/MMA bilayers on flexible kapton substrates, with overhanging generated via reactive ion etching (see SI section 1 for more details). A bridge 20-200 nm wide is first patterned between two electrodes and the kapton substrate is subsequently folded, breaking and stretching the nanocontact until it forms an atomic or nanoscale chain several atoms long. This technique has been successfully used both in magnetic and superconducting point contacts for spintronics and quantum computing studies.[20-22] In the case of Pt, it is predicted that as the number of atoms in the chain or the interatomic distance is increased, so is the magnetic moment.[1, 3] The actual conductance of a Pt atomic wire will depend on the exact orbital overlap, i.e. the bond between the atoms, or even the wire length.[2, 23] In addition to the atomic distances, it has been shown that the orbital overlap is also a function of the applied voltage and the chain configuration: linear or zigzag.[24, 25]

We have not observed any magnetic field dependent transport in Pt contacts at room temperature with conductance G in the range from 0.001 to 20 G_0 measured at 10^{-9}-10^{-3} mbar. However, at 4 K and for contacts with G close to G_0 (R ~ 12,900 Ω), we do measure a magnetic field dependent transport. The MR depends on the applied voltage, as apparent in samples which fluctuate between different resistance values (Fig. 1). In these samples, the nanostructure alternates between two similar resistance values at an applied voltage of 15 mV. The lower resistance state (~8.5 kΩ) shows a MR of -0.35%, but no MR was measured for the same

structure in the higher resistance state at the same voltage (~9.5 kΩ). Possible origins for the random telegraph fluctuations between different resistance/magnetic modes are a modified chain and interatomic distance due to atomic displacements,[5, 26, 27] voltage-induced instabilities in the orbital overlap,[24] or electron trapping/de-trapping processes.[28] At voltages of 50-60 mV or below -20 mV, the chain settles in a stable configuration with small fluctuations. Nevertheless, the resistance is different for positive and negative voltages. This could be explained as due to an asymmetric contact leading to different electric field profiles. The wire with the lowest resistance configuration exhibits the highest MR.

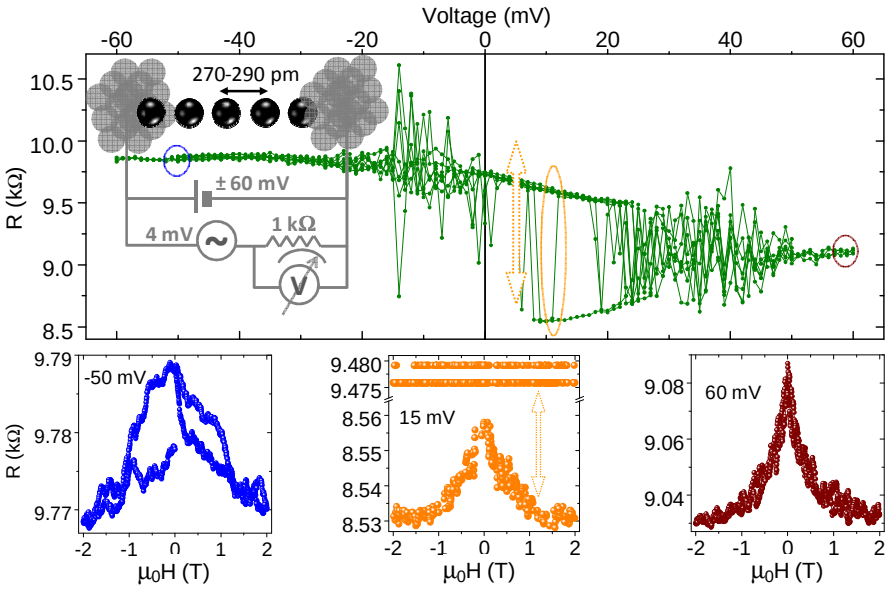

Figure 1. Resistance vs. voltage curve and MR for pure Pt atomic chains ≲1 nm long formed in high vacuum (10^{-8} mbar) and low temperatures (4.2 K). The resistance is measured using a 4 mV AC voltage. A superimposed DC voltage of up to +/- 60 mV changes the atomic configuration and/or orbital overlap (E ~ 10 MV/m). The random telegraph fluctuations are between two metastable states in the 5-25 mV range, one is dependent on magnetic field but the other is not. The schematic shows the measurement setup and a possible chain configuration according to the calculations in [1].

Oxygen cannot be ignored in experiments dealing with atomic structures that have not been fabricated and measured in ultra-high vacuum, as would usually be the case in devices for commercial applications. In Pt, the dissociation of O_2 molecules in situ with photons, conduction electrons, or heat leads to two oxygen atoms within two lattice constants of the original molecule with no diffusion of the chemisorbed molecules.[29] A local magnetic moment has been predicted in some amorphous Pt oxides,[30] so the presence of oxygen molecules need not be an obstacle for Pt nano-devices; it can extend their functionality and strengthen magnetic interactions.

Another benefit is that the presence of gas molecules greatly helps to stabilize the formation of nanostructures with a resistance in the tunneling regime,[31] where the distance between atoms and therefore the magnetic moments will be larger.[3] Achieving stable nanocontacts with large interatomic distances may be difficult due to vibrations, applied voltages, thermal fluctuations, etc. A dependence of the Fano factor with the conductivity in Pt atomic chains, i.e. an increased variation of the charge fluctuations with lower conductivities has previously been observed.[9, 32] Nevertheless, stable configurations with $G<G_0$ can be found in Pt nanocontacts connected by gas molecules.[14] Typical lifetimes for single atom and molecular contacts in break junctions are of the order of 1-100 s.[31, 33] We find that junctions formed in high vacuum (10^{-9}-10^{-8} mbar) with resistances of 0.1-100 MΩ tend to break after a few minutes at most, as shown in Fig. 2a. The transport at high resistances is also unstable, with noise fluctuations above 1% as we exceed 100 kΩ, see Fig. 2b. However, when air is allowed in the chamber to form a relatively low vacuum 10^{-5}-10^{-3} mbar, the contact is stabilized and can be measured for hours at a time with small resistance fluctuations (Fig. 2a). Junctions broken in this low vacuum show plateaux at large electrode distances of about 1 nm with a conductivity of 0.15 G_0 (85 kΩ) which are not observed in the high vacuum breaks – see the supplementary information (SI).

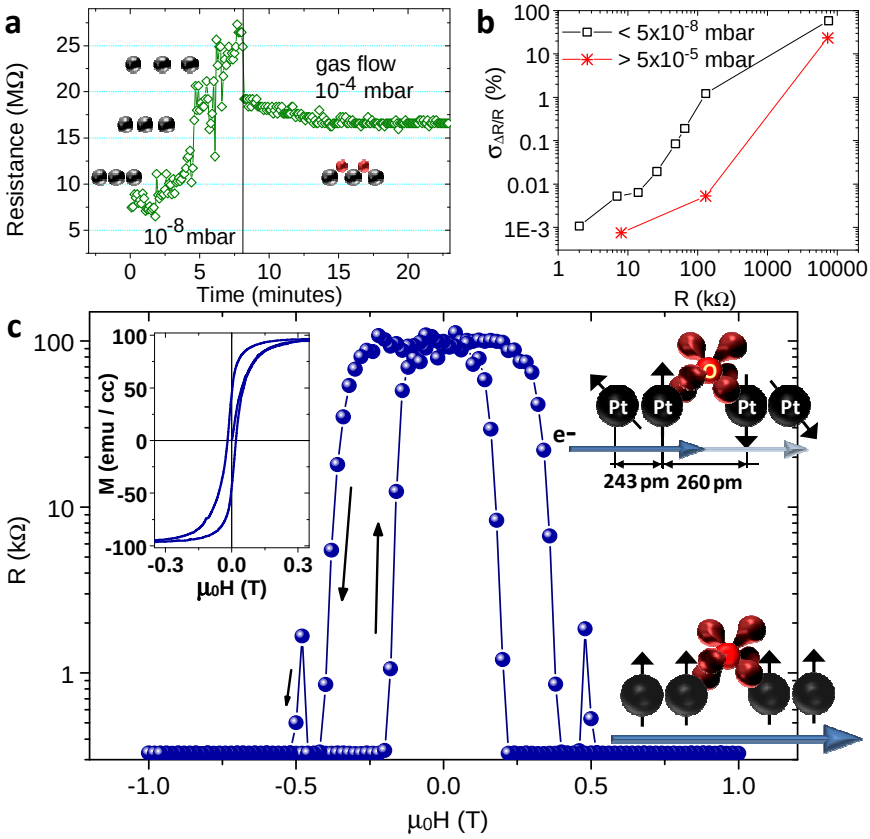

Figure 2. a. Resistance as a function of time in a Pt atomic chain measured in high and low vacuum. At high vacuum, the contact is breaking, going from 7 to 25 MΩ in 8 minutes. An air flow allows the stabilization of nanowires with R ~ 16 MΩ. **b.** Fluctuations of the resistance of Pt chains formed in high and low vacuum as a function of the resistance absolute value. At ~100 kΩ the peak to valley electrical noise is ±2 kΩ in high vacuum contacts compared to ±0.03 kΩ in low vacuum. **c.** MR in a Pt nanostructure formed under low vacuum conditions. The contact can measured for hours and has a MR of over 10,000%. The inset graph shows the magnetic moment per surface Pt atom for a [Pt/PtO_x]x5 multilayer (10 nm total thickness; raw data in Fig. S3).

Although these "dirty" contacts are stable over a wide range of resistances, they are particularly robust at ~100 kΩ, where resistance fluctuations are 3 orders of magnitude smaller than for pure Pt chains formed at high vacuum (Fig. 2b). The MR at temperatures ≤77 K in contacts formed

under low vacuum conditions is of up to -30,000% in fields of the order of 100 mT (Fig. 2c). The shape of the MR curve is also remarkable, as it is reminiscent of a bi-stable magnetic state system.[34, 35] Before a magnetic field is applied, the resistance for these contacts is of the order of 100 kΩ. However, the low resistance state under applied fields is of 100 Ω to 1 kΩ. This implies that the cross section of these structures must be a few atoms wide. Otherwise, the conductance quantization would result in higher resistance –even with all spin channels open the resistance of a Pt single atom chain cannot be below 3.2 kΩ.[5] Furthermore, the saturation field for these measurements is dependent on the measuring time: lower fields are needed in slower measurements (SI section 3). This can be attributed to the magnetic viscosity of the nanowires: at temperatures of 77 K or below the magnetization is dependent on thermally activated processes and results in spin dynamics comparable to the measurement time.[36, 37]

The highest MR ratios are measured at 77 K and 4.2 K in samples with initial resistance at zero field of ~100 kΩ. Other samples in the 1-200 kΩ range present as well very large negative MR values of 100-1000%. Differently from other magnetic oxide nanocontacts,[38] the MR changes sign as the resistance of the Pt nanostructures increases. Chains formed at low vacuum with a resistance over 200 kΩ have a positive MR of up to 6000% (Fig. 3).

The initial high resistance of all these samples points to tunneling rather than ballistic transport, but the huge MR and the sign changes are difficult to explain only in terms of spin polarized transport. It has been hypothesized that for pure Pt atomic chains, the spin-dependent effects may be quenched due to the low participation of the magnetic electrons in the transport.[9] By bonding the outer electrons, oxygen may contribute to enhance the contribution of the magnetic electrons to the charge transport. The magnetic ordering may also be favored by the presence of oxygen atoms in the nanostructures as, for example, in oxygen-deficient β-PtO_2.[30]

We indeed find that oxidized, 2 nm thick amorphous Pt thin films grown by sputter deposition can show ferromagnetic behavior with a small but measurable magnetization of up to 95 emu/cc (~0.08 μ_B per Pt atom), a remanence of 0.4-0.5 Ms and a coercive field of 20 mT at 2 K – see Fig. 2c. These samples were grown by sputter deposition. Samples with five repeats of 2 nm Pt layers were deposited (10 nm thick in total). Each layer was plasma oxidized at 2 torr O_2 atmosphere ($2x10^{-8}$ torr base) and 30 mA current. The results were compared to control samples of pure Pt (SI section 2).

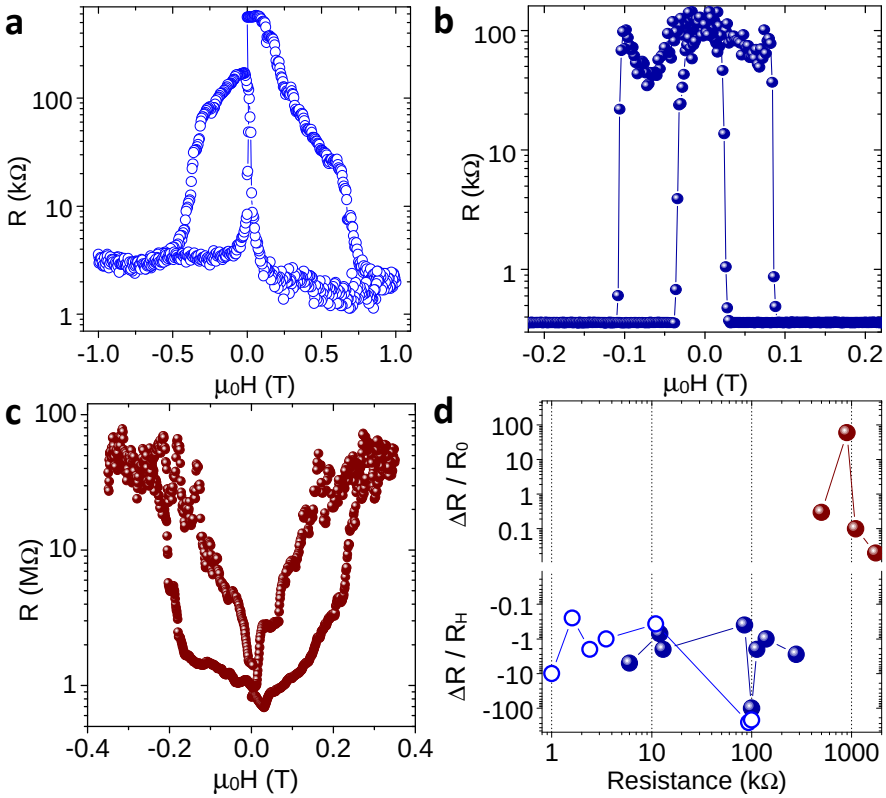

Figure 3. a-c. Large MR measured in gas-stabilized Pt nanowires with initial resistance R ≥100 kΩ measured at 4 K (a,c) and 77 K (b). Data in (c) averaged over 10 mT. **d.** Variation of the MR as a function of the nanowire resistance measured at 4 K (open symbols) and 77 K (filled symbols). The MR turns from negative (reduced resistance in a magnetic field – blue) to positive (increased resistance – red) for structures with resistance above ~300 kΩ.

In order to find a qualitative explanation for the enhanced MR in gas-stabilized contacts and the change in sign of the MR, we have performed density functional theory (DFT) calculations using the package Atomistix[39] (Fig. 4) in the revised generalized gradient approximation (revGGA; see SI).[40, 41] The lowest energy is found for a Pt-O-Pt atomic chain configuration when compared to other Pt-gas compounds. The oxygen atom is placed in between two Pt atoms, increasing the Pt-Pt equilibrium distance from 243 to 260 pm (Fig. 4). The atomic chains we simulate have metastable non-magnetic and magnetic configurations, where the simulations can converge from initial spin values of 0.01 and 0.5 μ_B. The magnetic state is on the order of 0.1 eV lower in energy, and the equilibrium Pt-O distance is increased from 198 to 218 pm when the Pt atoms are magnetized. Even though both states are relatively close in energy, they have different resistances. We may consider the magnetic field effect as stabilizing the magnetic configuration at finite temperature, which agrees with our experimental observation of two distinct resistance states. The MR may arise then from an enhanced contribution to the transport of spin polarized electrons,[9] as well as changes in magnetic ordering and orbital overlap with the magnetic field.[24]

Following this approach, we simulate the MR by calculating the electron current in structures with 4 Pt atoms at a fixed voltage of 10 mV at 77 K for initial spins of -0.01 μ_B/Pt (non-magnetic or disordered state with resistance R_0) and -0.5 μ_B/Pt (magnetic state with resistance R_H). The dependence of the electron transport calculated this way with the magnetic field agrees qualitatively with our measurements: changes in resistance from low to high spin states can be positive or negative depending on the configuration of the nanocontact. For example, the result is a MR of -89% for Pt chains with 2 oxygen atoms. However, if the chain is further pulled apart and 5 oxygen atoms can fit in the structure, the MR changes sign and becomes 104%, reproducing the sign change we observe experimentally, albeit for more resistive structures.

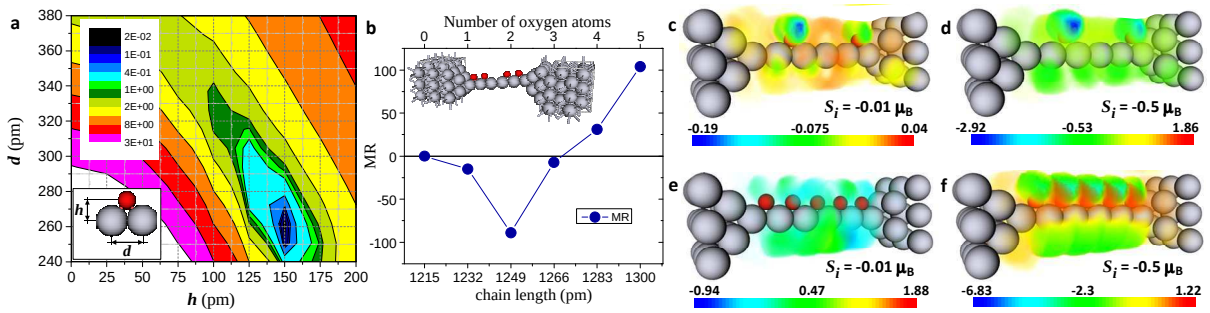

Figure 4. DFT-GGA simulations. **a.** Molecular energy of a Pt-O wire (color scale in eV). The ground state is obtained for a Pt-Pt distance *d* of 260 pm (compared to 243 pm without oxygen). The oxygen atom is at *h* = 150 pm above the Pt-Pt bond. **b.** We calculate the MR in an atomic chain 4 atoms long from the current flow for a fixed voltage of 10 mV as a function of the initial structural spin density: from -0.01 to -0.5 μ_B/atom. The inset shows the structure used for the calculations with 4 oxygen atoms (PtO). The simulated results show a change in the sign of the MR as we see in our experiments. **c-f.** Spin polarization densities (units of 0.1/Å^3) for wires with two (c-d) or five (e-f) oxygen atoms and an initial spin per Pt atom of -0.01 (c-e) or -0.5 μ_B (d-f).

Although the simulations predict a magnetic dependent transport and a change in the sign of the MR, they cannot reproduce the large effects we measure in some junctions. In order to explain the colossal MR ratios, we may need to consider spin orbit coupling (SOC) in larger nanostructures several atoms wide and the possibility of structural transition induced by the magnetic field. Our model does not include SOC, but it does predict a small displacement of the atoms in the magnetically aligned state. It has been demonstrated that a magnetic field can alter the atomic orbitals or structure of a magnetic atomic chain and drastically alter its resistance due to SOC.[17, 42, 43] Furthermore, small Pt clusters have strong SOC[16] leading to anisotropic effects in magnetic atoms,[44] suggesting that the SOC interaction could induce larger structural changes and play an important role in the magnitude of the MR effect.

The potential of extremely large magnetoresistive ratios and the high stability of our gas-formed Pt junctions include applications in quantum computing to detect the highly localized fields of qubits or other nanostructures. Furthermore, the ability to tune the spin states and the sign of the resistance change in atomic structures via magnetic and electric fields opens paths of research for "dirty" quantum operators that work at ambient pressures. Further research could also be carried out to investigate the use of magnetic fields in the speed of chemical reactions with nanostructured PtO_2 –commonly known as Adams's catalyst.[45]

Associated content: Additional information and figures on fabrication method, magnetometry and magnetoresistive measurements and DFT simulations.

Author information:

Corresponding author: E-mail: o.cespedes@leeds.ac.uk (O.C.).

Acknowledgements: We wish to thank Drs. Steven Achilles, Martin Gratland, Javier Ferrer, Alexander Smogunov, Cyrille Barreteau and Erio Tosatti for advice on the origin of the MR effects and calculation methods.

Funding sources: We are grateful to EPSRC for support via the grant EP/K00512X/1.

References:

1. Delin, A.; Tosatti, E. *Physical Review B* **2003,** 68, (14).
2. de la Vega, L.; Martin-Rodero, A.; Yeyati, A. L.; Saul, A. *Physical Review B* **2004,** 70, (11).
3. Delin, A.; Tosatti, E. *Surface Science* **2004,** 566, 262-267.
4. Smogunov, A.; Dal Corso, A.; Delin, A.; Weht, R.; Tosatti, E. *Nature Nanotechnology* **2008,** 3, (1), 22-25.
5. Delin, A.; Tosatti, E. *Journal of Physics-Condensed Matter* **2004,** 16, (45), 8061-8074.
6. Rodrigues, V.; Bettini, J.; Silva, P. C.; Ugarte, D. *Physical Review Letters* **2003,** 91, (9).
7. Li, C. Z.; He, H. X.; Bogozi, A.; Bunch, J. S.; Tao, N. J. *Applied Physics Letters* **2000,** 76, (10), 1333-1335.
8. Untiedt, C.; Dekker, D. M. T.; Djukic, D.; van Ruitenbeek, J. M. *Physical Review B* **2004,** 69, (8).
9. Kumar, M.; Tal, O.; Smit, R. H. M.; Smogunov, A.; Tosatti, E.; van Ruitenbeek, J. M. *Physical Review B* **2013,** 88, (24).
10. Schmaus, S.; Bagrets, A.; Nahas, Y.; Yamada, T. K.; Bork, A.; Bowen, M.; Beaurepaire, E.; Evers, F.; Wulfhekel, W. *Nature Nanotechnology* **2011,** 6, (3), 185-189.
11. Mahato, R. N.; Lulf, H.; Siekman, M. H.; Kersten, S. P.; Bobbert, P. A.; de Jong, M. P.; De Cola, L.; van der Wiel, W. G. *Science* **2013,** 341, (6143), 257-260.
12. Guedon, C. M.; Valkenier, H.; Markussen, T.; Thygesen, K. S.; Hummelen, J. C.; van der Molen, S. J. *Nature Nanotechnology* **2012,** 7, (5), 304-308.
13. Ienaga, K.; Nakashima, N.; Inagaki, Y.; Tsujii, H.; Kimura, T.; Kawae, T. *Applied Physics Letters* **2012,** 101, (12).
14. Tal, O.; Kiguchi, M.; Thijssen, W. H. A.; Djukic, D.; Untiedt, C.; Smit, R. H. M.; van Ruitenbeek, J. M. *Physical Review B* **2009,** 80, (8).
15. Szyja, B. M.; Huu Chuong, N.; Kosov, D.; Doltsinis, N. L. *Journal of Molecular Modeling* **2013,** 19, (10), 4173-4180.
16. Blonski, P.; Dennler, S.; Hafner, J. *Journal of Chemical Physics* **2011,** 134, (3).
17. Shi, S. F.; Ralph, D. C. *Nature Nanotechnology* **2007,** 2, (9), 522-522.
18. Yanson, A. I.; Bollinger, G. R.; van den Brom, H. E.; Agrait, N.; van Ruitenbeek, J. M. *Nature* **1998,** 395, (6704), 783-785.
19. Xiang, D.; Jeong, H.; Lee, T.; Mayer, D. *Advanced Materials* **2013,** 25, (35), 4845-4867.
20. Egle, S.; Bacca, C.; Pernau, H.-F.; Huefner, M.; Hinzke, D.; Nowak, U.; Scheer, E. *Physical Review B* **2010,** 81, (13), 134402.
21. Zgirski, M.; Bretheau, L.; Le Masne, Q.; Pothier, H.; Esteve, D.; Urbina, C. *Physical Review Letters* **2011,** 106, (25).
22. Viret, M.; Berger, S.; Gabureac, M.; Ott, F.; Olligs, D.; Petej, I.; Gregg, J. F.; Fermon, C.; Francinet, G.; Le Goff, G. *Physical Review B* **2002,** 66, (22).
23. Autes, G.; Barreteau, C.; Spanjaard, D.; Desjonqueres, M.-C. *Physical Review B* **2008,** 77, (15).
24. Nielsen, S. K.; Noat, Y.; Brandbyge, M.; Smit, R. H. M.; Hansen, K.; Chen, L. Y.; Yanson, A. I.; Besenbacher, F.; van Ruitenbeek, J. M. *Physical Review B* **2003,** 67, (24).
25. Vardimon, R.; Yelin, T.; Klionsky, M.; Sarkar, S.; Biller, A.; Kronik, L.; Tal, O. *Nano Letters* **2014,** 14, (6), 2988-2993.

26. Ralls, K. S.; Ralph, D. C.; Buhrman, R. A. *Physical Review B* **1993,** 47, (16), 10509-10514.
27. Cespedes, O.; Jan, G.; Viret, M.; Bari, M.; Coey, J. M. D. *Journal of Applied Physics* **2003,** 93, (10), 8433-8435.
28. Raghavan, N.; Degraeve, R.; Fantini, A.; Goux, L.; Strangio, S.; Govoreanu, B.; Wouters, D. J.; Groeseneken, G.; Jurczak, M.; Ieee. *2013 Ieee International Reliability Physics Symposium (Irps)* **2013**.
29. García-Suárez, V. M.; Rocha, A. R.; Bailey, S. W.; Lambert, C. J.; Sanvito, S.; Ferrer, J. *Physical Review B* **2005,** 72, (4), 045437.
30. Yang, Y.; Sugino, O.; Ohno, T. *Physical Review B* **2012,** 85, (3).
31. Tsutsui, M.; Taniguchi, M.; Kawai, T. *Nano Letters* **2008,** 8, (10), 3293-3297.
32. Kumar, M.; Smit, R. H. M.; van Ruitenbeek, J. M.; Tal, O. *2011 21st International Conference on Noise and Fluctuations (Icnf)* **2011**, 376-380.
33. Tsutsui, M.; Shoji, K.; Taniguchi, M.; Kawai, T. *Nano Letters* **2008,** 8, (1), 345-349.
34. Prezioso, M.; Riminucci, A.; Bergenti, I.; Graziosi, P.; Brunel, D.; Dediu, V. A. *Advanced Materials* **2011,** 23, (11), 1371-1375.
35. Sokolov, A.; Sabirianov, R.; Sabirianov, I.; Doudin, B. *Journal of Physics-Condensed Matter* **2009,** 21, (48).
36. George, R. G. *Nature* **1959,** 183, (4656), 245-245.
37. Sellmyer, D. J.; Zheng, M.; Skomski, R. *Journal of Physics-Condensed Matter* **2001,** 13, (25), R433-R460.
38. Cespedes, O.; Clifford, E.; Coey, J. M. D. *Journal of Applied Physics* **2005,** 97, (6).
39. Brandbyge, M.; Mozos, J. L.; Ordejon, P.; Taylor, J.; Stokbro, K. *Physical Review B* **2002,** 65, (16).
40. Perdew, J. P.; Burke, K.; Ernzerhof, M. *Physical Review Letters* **1996,** 77, (18), 3865-3868.
41. Zhang, Y. K.; Yang, W. T. *Physical Review Letters* **1998,** 80, (4), 890-890.
42. Viret, M.; Gabureac, M.; Ott, F.; Fermon, C.; Barreteau, C.; Autes, G.; Guirado-Lopez, R. *European Physical Journal B* **2006,** 51, (1), 1-4.
43. Bolotin, K. I.; Kuemmeth, F.; Pasupathy, A. N.; Ralph, D. C. *Nano Letters* **2006,** 6, (1), 123-127.
44. Gambardella, P.; Rusponi, S.; Veronese, M.; Dhesi, S. S.; Grazioli, C.; Dallmeyer, A.; Cabria, I.; Zeller, R.; Dederichs, P. H.; Kern, K.; Carbone, C.; Brune, H. *Science* **2003,** 300, (5622), 1130-1133.
45. Voorhees, V.; Adams, R. *Journal of the American Chemical Society* **1922,** 44, 1397-1405.